Copper, Iron and Zinc Removal Using Doum Palm (*Hyphaene Thebaica*) Kernel as Biosorbent

Samuel K. Caleb, Idris M. Muhammad, Jibril Mohammed
Abubakar Tafawa Balewa University, Bauchi, Bauchi State, Nigeria

Abstract: **- Wastewater produced from pre-tanning operations in Gombe pre-tannery is directly discharged into the environment resulting in the release of heavy metal ions which when present above required limits pose health hazards. In this work, Doum palm kernel, an agricultural waste was used for the adsorption of copper, iron and zinc ions from Gombe pre-tannery wastewater. The Doum palm kernels were prepared using standard methods and characterized for elemental and oxide composition, functional groups, surface morphology and surface area using X-Ray Flourescence, Fourier Transform Infra-Red, Scanning Electron Microscopy and Brunuaer, Emmet and Teller analytical equipment respectively. The XRF results showed 43.4% K, 18.1% Ag, 13.2% among others with the highest being potassium (K) of 43.4% and a corresponding oxide concentration of 34.1%. Biosorption studies with the kernel showed that it can be used in the reduction of copper, iron and zinc ions with 4.2g doum palm kernel per liter of Gombe pre-tannery wastewater at an equilibrium time of 30 minutes with 57.33%, 54.84% and 98.76% removal for copper, iron and zinc ions respectively. Mixing speed and temperature effects were also studied. Adsorption data were tested using Langmuir, Freundlich and Temkin models. Different error analyses reveal that experimental data fit Temkin for copper, Freundlich for iron and Langmuir isotherm for zinc. Adsorption kinetic models reveal second-order kinetics with chemisorption being the rate limiting step. Thermodynamic results show enthalpy (ΔH) of -52.1 kJ/mol and entropy (ΔS) of -0.174 kJ/mol for Copper, while ΔH and ΔS for iron were -52.9 kJ/mol and -0.181 kJ/mol respectively. ΔH and ΔS for zinc were + 20.7 kJ/mol and +0.066 kJ/mol for zinc respectively. ΔG values for Copper and iron at 50 ^{0}C (-4318 kJ and -5590 kJ) shows non-spontaneous sorption while that of zinc (+602 kJ) shows spontaneous sorption.**

Keywords: **Doum palm kernel, pre-tannery wastewater, biosorption, kinetic models, thermodynamics**

I. INTRODUCTION

Water is considered to be a vital and limited resource; population growth, industrial development and other pressures faced by developing countries have led to structured measures to ensure sustainable management of this important resource (Addagalla, *et al.,* 2009). There are various sources of water like ponds, lakes, rivers, dams etc. available for the use of industrial, domestic and agricultural purposes. These water bodies get polluted due to the discharge of effluents from industries, domestic waste, land and agricultural drainage resulting in the degradation of this water resource (Chakraborty *et al.,* 2005). Due to toxic effects of particular elements on the environment and bioaccumulation in the food chain, heavy metals pose serious threats to living organisms (Filipiuk, *et al.,* 2006). Copper and iron can be obtained by ingestion and dermal contact. They are beneficial micro-nutrients essential to the body when in its organic forms as in food. Health effects of excessive copper and iron in the body include Alzheimer's type II disease which is a result of elevated free copper and iron levels in the body, astrocytosis, Parkinsonism, cognitive dysfunction and ataxia (Butterworth, 2010; Mercer, 2001; Faller, 2009; Hureau and Faller, 2009, Butterworth, 2010). Iron is the most abundant transition metal in the earth's crust. Biologically it is the most important nutrient for most living creatures as it is the cofactor for many vital proteins and enzymes. Iron mediated reactions support most of the aerobic organisms in their respiration process. If it is not shielded properly, it can catalyze the reactions involving the formation of radicals which can damage biomolecules, cells, tissues and the whole organism. Iron poisoning has always been a topic of interest mainly to pediatricians (Monisha*et al.,*2014). It can also cause accumulation in muscle, liver and fish gills (Visnjic-Jeftic *et al.,* 2010) as well as negative effects on brain and central nervous functions (Struzynska, 2009). Zinc is one of the most important metals often found in effluents discharged from industries involved in acid mine drainage, tanning, galvanizing plants, natural ores and municipal wastewater treatment plants. It is not biodegradable and travels through the food chain via bioaccumulation. Toxicity of zinc has several reversible and irreversible effects on natural flora and fauna. For example, very low exposure to zinc is responsible for gastrointestinal disturbance i.e. irritability, nausea, loss of appetite, metal fume fever and muscular stiffness (Lesmana *et al.,*2009; Bhattacharya Mandal and Das*,* 2006; Vilar*et al.,* 2007; Marin and Ortuno *et al.,* 2009).

Biosorption is a physicochemical process that binds ions of metals (that are mostly present in the form of cations) by cell membranes, i.e. by compounds with negative charge that are present in cell membranes. It has distinct advantages over conventional methods of treatment, as this process does not produce secondary chemical sludge, hence no secondary pollution, more efficient, ecofriendly and easy to operate (Norton *et al.,* 2004; Mishra, 2014). The biosorbents are readily available and they are quite efficient to remediate heavy metals below a threshold concentration of 100 mg/L. More so, in biosorption, the use of microorganisms does not involve the supply of nutrients. Thus, the process of

biosorption is extensively simple and does not require skilled labor (Mishra, 2014). The biggest advantage of biosorption is that heavy metals are bound by cells that no longer show metabolic activity. This allows for removal of contaminant by dead organisms, and thus the process is simpler and less expensive because supporting living biomass requires an additional supply of nutrients and energy (Babak *et al.,* 2012; Ahalya *et al.,* 2003).

The study aims to investigate the adsorption of Cu^{2+}, Fe^{2+} and Zn^{2+} ions from Gombe pre-tannery wastewater onto a readily available agricultural by-product, Doum palm seed kernel. The effect of dosage, reaction time, mixing speed and temperature on the efficiency of biosorption of the above metal ions were also analyzed. The Langmuir, Freundlich and Temkin models were utilized for analysis of the adsorption equilibrium. Kinetic models were tested to identify the potential adsorption process mechanisms. Characterization of the biosorbent was made using XRF, FTIR, SEM and surface area measurement using nitrogen adsorption technique by BET method. Thermodynamic analyses were also done to identify the energy and heat changes in the adsorption process.

II. MATERIALS AND METHOD

A. Materials

Doum palm fruits were collected from Gombe main market, Gombe, Nigeria. The wastewater was obtained from Gombe pre-tannery/abbatoir. The solvent, petroleum ether 75/80 was obtained from Marcy Surgicals, Gombe-Nigeria. All chemicals and reagents were of analytical grade. Distilled water was obtained from Gubi Dam Water Treatment Plant Laboratory and Civil and Environmental Engineering Laboratory, ATBU all in Bauchi State-Nigeria. The fruits were crushed to remove the kernels which were then size reduced and dried using a GenLab MIN0/100 Y6G134 (manufactured in the USA) oven until constant weight. The dried kernels were then ground using a laboratory mortar and pestle and then sieved. A Sigma-Aldrich CLX3740XL Soxhlet machine was used to extract oil from the sample. A Minipal-4 XRF machine was used to identify the elements and elemental oxides present in the sample and their percentage amounts. A Shimadzu 8400S FTIR spectrometer with wave numbers 4000-500cm^{-1} was also used to identify functional groups in the sample. Scanning electron microscopy was done by a VPSEM SUPRA 35VP (Manufactured by Zeiss) to identify surface morphology and textural formation of the sample. The porosity, surface area and pore characteristics was measured by a V-Sorb 2800 BET machine. The pre-tannery wastewater was characterized for presence and concentration of copper and iron (II) ions by a Wagtech 7100 photometer while a BUCK 210AA (by Buck Scientific USA) Atomic Adsorption Spectrophotometer was used to test for the presence of zinc ions.

B. Method

The doum palm fruits were crushed and washed in order to remove the fleshy rind enclosing the hard kernel. The hard shells were then broken to get its kernel used for this research. The *Hyphaenethebaica* kernels were broken into pieces, washed with deionized water, sundried and oven dried at 60^0C for 24 hours.

C. Moisture Content

100g of the kernels was weighed using a digital weighing balance. This formed the initial weight W_1. The sample was then placed in an oven to dry at a temperature of 70^0C for one-hour after which the sample was re-weighed. The entire process was repeated until constant weight was achieved. This constant weight was then designated W_2. The moisture content of each set of oven dried kernels was determined on average weight basis and expressed in percentage using the formula

$$\text{Moisture content (\%)} = \frac{W_2 - W_1}{W_1} X100 \qquad (1)$$

Where

W_1= initial weight of sample (g)

W_2= oven dried (constant) weight (g)

D. Oil Content and Cake recovery

The dried kernels were then ground to increase their surface area using a mortar and pestle. 100g of each set of ground kernels was weighed and put into the Soxhlet extractor where extraction was carried out for about four hours using petroleum ether as solvent at a temperature of 75^0C. The cake sample was then extracted, dried and weighed again. The extracted oil was weighed and kept. The average percentage yield was obtained using the same equation (1) only that the initial weight (W_1=100g) and the weight of cake after extraction of the oil were completed, washed with de-ionized water until free of solvent and then oven dried at 70^0C until constant weight (W_2).

E. Characterization of the biosorbent

The biosorbent was characterized using XRF, FTIR, SEM and BET methods to obtain the elemental and oxide composition, functional groups, surface morphology and the pore characteristics of the biosorbent.

F. Characterization of the pre-tannery wastewater

1). Sample collection: A 25-L sample of pre-tannery wastewater was obtained from Gombe abattoir/tannery. Out of this, 10ml was taken and analyzed for physico-chemical parameters such as turbidity, pH, temperature, conductivity as well as the initial concentrations of zinc, copper and iron metal ions using a spectrophotometer.

2). Jar test: Jar test was conducted using flocculator on Gombe pre-tannery wastewater to determine the optimum parameters (dosage, mixing speed, mixing time, temperature) of the doum palm kernel that will give desired results. 600ml of the pre-tannery wastewater sample was measured and poured into five different beakers. For optimum dosage, different amounts of biosorbent was poured into the beakers. The stirring paddles were then lowered into the beakers and the jar test machine turned on and operated at a speed of 100rpm for 30min. The beakers were then withdrawn, filtered and analyzed for the uptake of copper, iron and zinc ions from the water by the various masses of doum palm kernel powder. Each concentration was recorded and percentage metal removed was calculated using Equation 2:

$$\frac{C_0 - C_1}{C_0} \text{ X } 100 \qquad \ldots (2)$$

Where C_o – Initial concentration of copper, iron and zinc in the pre-tannery wastewater (mg/L).

C_1 – Concentration of metal ion after treatment by doum palm kernel powder of different masses (mg/L).

The dosage (in grams) which gave the highest and constant percentage removal of copper, iron and zinc ions was taken as the optimum dosage. For optimum time, the optimum dose was poured into five different beakers containing the same volume of pre-tannery wastewater and placed in the machine one after the other with the time of each set at 5min intervals beginning from 10min and ending at 30min. The beakers were each withdrawn, filtered and analyzed for the uptake of copper, iron and zinc ions. For optimum speed, the same process was used for optimum time only with the speed being varied from 50rpm, 100rpm, 150rpm, 200rpm and 300rpm for each beaker with the optimum time and dosage set. For optimum temperature, each of the five beakers was filled with the same volume of liquid and the optimum dosage poured in. Each beaker was placed in a water bath with the temperature set at 30^0C using a thermometer. Each of the mixtures were stirred at the optimum speed and kept in the bath for the optimum time but at different temperatures of 35^0C, 40^0C, 45^0C and 50^0C. The beakers were withdrawn and analyzed for the uptake of copper, iron and zinc ions using Eqn. (2). The data obtained from the experimental procedures above were used in calculating the concentration of copper, iron and zinc retained in the adsorbent as presented in Equation (2) (Lam and Zakaria, 2008; Sugumaran *et al.,* 2012). The quality of copper, iron and zinc metal ions in the adsorbent phase is determined by;

$$q_t = \frac{(C_0 - C_t)V}{m} \qquad \ldots (3)$$

Where;

q_t = amount of adsorbed copper, iron and zinc on adsorbent surface (mg/g) at time t,

C_0 = initial concentration of copper, iron and zinc ions in solution (mg/L): 1.5, 3.1 and 0.81mg/L respectively,

C_t = concentration of copper, iron and zinc in solution at each time of adsorption (mg/L)

V = Volume of wastewater (L) = 0.6 L

m = mass of biosorbent = 2.5g

The equilibrium adsorption capacity q_e (mg/g) at different concentrations is expressed as;

$$q_e = \frac{(C_0 - C_e)V}{m} \qquad \ldots (4)$$

Where

C_e: final concentration of copper, iron and zinc ions in solution (mg/L).

C_e is the maximum the biosorbent attained in the removal of copper, iron and zinc from Gombe pre-tannery wastewater

Percentage removal of copper, iron and zinc ions is given by

$$\%\text{removal} = \frac{(C_0 - C_t)}{C_0} \text{ X } 100 \qquad \ldots (5)$$

It is to be noted that C_o, C_t and C_e (mg/L) are the liquid phase concentrations of sorbate at initial, time and equilibrium respectively.

G. Thermodynamic Analysis

In practice, thermodynamic parameters are very important and can be taken into consideration to evaluate the spontaneity or otherwise of the biosorption process. The equilibrium amount of copper, iron and zinc adsorbed onto the doum palm kernel at different temperatures was examined to obtain thermodynamic parameters such as standard Gibbs free energy change (ΔG^0), standard enthalpy change (ΔH^0), and standard entropy change (ΔS^0) (Huang *et al.,* 2011). Using the Van't Hoff equation,

$$\Delta G^0 = \Delta H^0 - T\Delta S^0 = RT\ln K_c \qquad \ldots (6)$$

Where

$$K_c = \frac{q_e}{C_e} \qquad \ldots (7)$$

And

$$\ln K_c = -\frac{\Delta H^0}{RT} + \frac{\Delta S^0}{R} \qquad \ldots (8)$$

K_e is the equilibrium constant, q_e is the amount of copper, iron and zinc ions adsorbed at equilibrium (mg/g), C_e is the equilibrium copper, iron and zinc concentration in

solution (mg/L), R is the universal gas constant (8.314 x 10^{-3}kJ $mol^{-1}K^{-1}$), T is the absolute temperature (K). ΔH^0, ΔS^0 and ΔG^0 are the standard enthalpy (kJ/mol), standard entropy (kJ $mol^{-1}K^{-1}$) and Gibb's free energy (Adekola *et al.,* 2016; Tan *et al.,* 2012).

The enthalpy and entropy were obtained as the slope and intercept of the linearized form of Equation (8) obtained from the graph of ln K_c against 1/T while the Gibb's free energy was obtained at different temperatures (298K to 323K).

H. Adsorption Isotherms

Langmuir, Freundlich and Temkin isotherms were used to model the design using linearized equations (9) - (12) (El-Sadaawy and Abdelwahab, 2014; Hameed *et al.,* 2009; Muhammad *et al.,* 2012)

1) Langmuir Isotherm: The Langmuir isotherm assumes monolayer adsorption on a uniform surface with a finite number of adsorption sites. Once a site is filled, no further sorption can take place at that site. As such the surface will eventually reach a saturation point where the maximum adsorption of the surface will be achieved. The Langmuir adsorption isotherm equation was initially developed to describe the adsorption of gases onto clean solids. It is often used to describe the sorption of solute from solution. This equation can be derived theoretically based on evaporation and condensation rates. Based on ideal assumption of a monolayer, adsorption of adsorbate on adsorbent surface the Langmuir isotherm model (Langmuir, 1918)is expressed in linear form as follows:

$$\frac{1}{q_e} = \left(\frac{1}{K_L Q_m}\right)\frac{1}{C_e} + \frac{1}{Q_m} \quad \dots (9)$$

where Q_m is the maximum monolayer adsorption capacity (mg/g) and K_l is the Langmuir constant which is related to the heat of adsorption (L/mg). The essential features of the Langmuir isotherm can be expressed in terms of the dimensionless separation factor (R_L) given by (Hall and Eagleton *et al.,* 1966):

$$R_L = \frac{1}{(1 + K_l C_o)} \quad \dots (10)$$

The value of separation factor R_L indicates either the adsorption isotherm to be unfavorable ($R_L > 1$), favorable ($0 < R_L > 1$), linear ($R_L = 1$) or irreversible ($R_L = 0$).

2). *Freundlich Isotherm*: Freundlich presented the earliest known sorption isotherm equation (Freundlich, 1906). This empirical model has been applied to non-ideal sorption on heterogeneous surfaces as well as multilayer sorption (Awwad and Salem, 2011). The Freundlich isotherm model is the well-known earliest relationship describing the adsorption process. This model applies to adsorption on heterogeneous surfaces with the interaction between adsorbed molecules. The application of the Freundlich equation also suggests that sorption energy exponentially decreases on completion of the 'sorptional centers' of an adsorbent. This isotherm is an empirical equation and can be employed to describe heterogeneous systems and is expressed as follows:

$$\ln q_e = \ln K_F + \frac{1}{n_F}\ln C_e \dots (11)$$

The Freundlich equation is strictly valid only for ion adsorption at low concentration. The Freundlich isotherm has been derived by assuming an exponentially decaying sorption site energy distribution. It is often criticized for lacking a fundamental thermodynamic basis since it does not reduce to Henry's law at low concentrations.

3).Temkin Isotherm: The Temkin isotherm equation assumes that the fall in the heat of adsorption of all the molecules in the layer decreases linearly with coverage due to adsorbent–adsorbate interactions, and that the adsorption is characterized by a uniform distribution of the binding energies up to some maximum binding energy (Aharoni and Ungarish 1977). This isotherm takes into accounts of indirect adsorbate-adsorbate interactions on adsorption isotherms. Temkin noted experimentally that heats of adsorption would more often decrease than increase with increasing coverage. The Temkin isotherm can be described in the following equation,

$$q_e = B_T \ln A + B_T \ln C_e \quad \dots (12)$$

Where

$$B_T = (RT)/b_T \quad \dots (13)$$

where K_T is the equilibrium binding constant (L mol^{-1}) corresponding to the maximum binding energy, b is related to the adsorption heat, R is the universal gas constant (8.314 J $K^{"1}$ $mol^{"1}$) and T is the temperature (K). Plotting q_e versus ln (C_e) (Equation (5)) results in a straight line of slope RT/b and intercept (RT ln K_T)/b. The Temkin isotherm assumes that the heat of adsorption of the molecules in a layer decreases linearly due to adsorbent–adsorbate interaction and that the binding energies are uniformly distributed (Reddy *et al.*, 2010).

I. Adsorption Kinetics

Kinetic studies are required to find out the rate and mechanism of reaction coupled with determination of rate controlling step (Mishra, 2014). The study of kinetic models also helps in the design of continuous adsorption columns (Basha*et al.,* 2009). Adsorption kinetics is one of the most important data used in order to understand the mechanism of adsorption and to assess the performance of the adsorbent. The experimental data for adsorption kinetics were studied using three models namely: Lagergren pseudo-first order kinetics, Lagergren pseudo-second order kinetic and the intra-particle diffusion models respectively (Hameed, *et al.,* 2009; El-Nafaty, Muhammad *et al.,* 2012; El-Sadaawy and

Abdelwahab, 2014). The linearized form of the equations are as follows:

1). *Pseudo-first order equation*: The Lagergren's rate equation is one of the most widely used rate equations to describe the adsorption of an adsorbate from the liquid phase. This model assumes the presence of physical forces of attraction between adsorbate and adsorbent particles. The binding of adsorbate with adsorbent is reversible and non-dissociative. The model also considers that the rate of binding of adsorbate species with adsorbent particles is directly proportional to the number of vacant active sites present on the surface of adsorbent. The linear form of pseudo-first order equation is given as:

$$\log(q_e - q_t) = \log q_e - \frac{k_1}{2.303} t \quad \ldots (14)$$

2). *Pseudo-second order rate equation (PSOE)*: The application of PSOE includes the systems containing various kinds of sorbates (heavy metals in both cationic and anionic forms, organic dyes, phenols, etc.) and sorbents (inorganic minerals, activated carbons, raw biomass, etc.). The good applicability of this equation is usually associated with the situation when the rate of direct adsorption/desorption process (seen as a kind of chemical reaction further referred to as 'surface reaction') controls the overall sorption kinetics (Plazinski*et al.,*2009). The linear form of the pseudo-second-order model is given by the following equation (Ho and McKay 1999; Ho, 2006a)

$$\frac{t}{q_t} = \frac{1}{k_2 q_e^2} + \frac{t}{q_e} \quad \ldots (15)$$

3). *Intra-particle diffusion model*: Diffusion models were also employed to describe the copper, iron and zinc adsorption process. Three main steps are involved in the solid–liquid sorption process between the metal ions and the adsorbent (Kalavathy*et al.,* 2005);

a) The metal ions are transferred from the bulk solution to the external surface of the adsorbent. This is known as film diffusion,
b) The metal ions are transferred within the pores of the adsorbent. This is known as intra-particle diffusion, occurring either as pore diffusion or as a solid surface diffusion mechanism,
c) The active sites on the surface of the adsorbent capture the metal ions.

The intra-particle diffusion model is given by the following equation (Weber and Moriss, 1963)

$$q_t = K_{dif} t^{1/2} + C \quad \ldots (16)$$

Where q_e is amount of copper, iron and zinc ions adsorbed at equilibrium, q_t is the amount of copper, iron and zinc ions adsorbed at time t. K_{dif} is the diffusion constant

J. Error Functions and Optimization of Kinetics

Due to the inherent bias resulting from linearization, alternative isotherm parameter sets were determined by non-linear regression showing a mathematical method for determining isotherm parameters using the original form of the isotherm equation. In the single component isotherm studies, the optimization procedure requires an error function to be defined in order to be able to evaluate the fit of the isotherm to the experimental equilibrium data (Chan *et al.,* 2012). In this study, five different error functions were examined to validate the linear regression (R^2) coefficient as shown from Equations (17-21).

1. The Average Percentage Error (APE)

$$\text{APE}(\%) \frac{100}{N} \times \sum_{i=1}^{N} \left[\frac{q_{e,isotherm} - q_{e,exp}}{q_{e,isotherm}}\right] i \quad \ldots (17)$$

2. Chi-square test statistic (χ^2)

$$\chi^2 = \sum_{i=1}^{N} \frac{(q_{e,isotherm} - q_{e,exp,})^2}{q_{e,isotherm}} \quad \ldots (18)$$

3. Marquadt's Percent Standard Deviation (MPSD)

$$\text{MPSD} = 100 \times \sqrt{\frac{1}{N-P} \sum_{i=1}^{N} \frac{(q_{e,isotherm} - q_{e,exp})_i^2}{q_{e,isotherm}}} \ldots (19)$$

4. Root Mean Square (RMS) error

$$\text{RMS} = 100 \times \sqrt{\frac{1}{N} \sum_{i=1}^{N} \left(1 - \frac{q_{e,exp}}{qe,isotherm}\right)^2} \ldots (20)$$

5. Root-Mean-Square-Deviation (RMSD)

$$\text{RMSD} = \sqrt{\frac{1}{N} \sum (q_{e,exp} - q_{e,isotherm})^2} \quad \ldots (21)$$

Where $q_{e,\,exp}$ are the experimental values of q_e, mg/g, $q_{e,\,isotherm}$ are the calculated values of q_e from the linear relationship, *N* is the number of data points and *p* is the number of degrees of freedom.

III. RESULTS AND DISCUSSIONS

A. Characterization of the biosorbent

1).*Morphology Analysis*: In order to get an idea of the microscopic structure of the biosorbent surface and estimate the biosorption mechanisms, the surface of doum palm kernel was determined by magnification. The morphology of the doumpalm kernel powder as shown below shows that the biosorbent surface is irregular and rough with the presence of voids, crevices, troughs and cavities (which very likely play a major role in biosorption and intra-particle diffusion). The presence of voids and pores on the surface of doumpalm kernel reveals the possibility of copper, iron and zinc ion accumulation as suggested by Pohkre and Viraraghavan (2008). The morphology as shown is characteristic of doumpalm kernel.

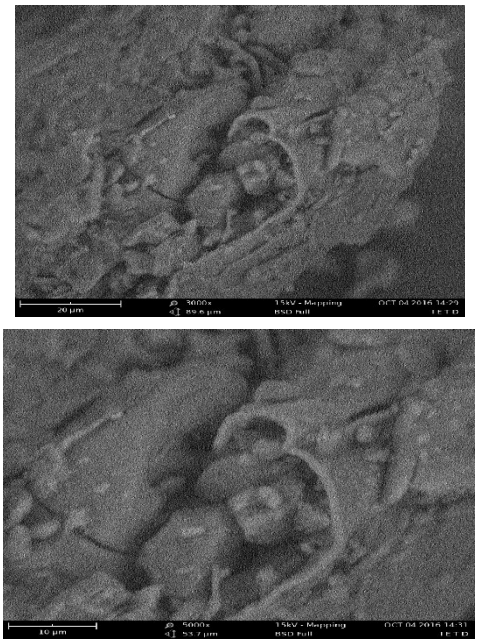

Fig 1. Scanning Electron Micrograph of doum palm kernel under 50µm and 20µm magnification

2). FTIR Analysis: The FTIR analysis of Doum palm kernel is shown below

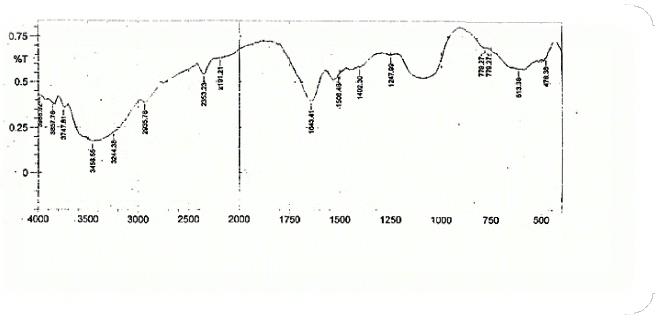

Fig 2. Fourier Transform Infra-Red (FTIR) spectra for doum palm kernel

From the FTIR spectral analysis it was observed that there was a broad and intense absorption peak around the 3456.55cm^{-1} corresponding to the O-H stretching vibrations due to inter- and intra-molecular hydrogen bonding of polymeric compounds (macromolecular associations), such as alcohols, phenols and carboxylic acids, as in pectin, cellulose and lignin, thus showing the presence of "free" hydroxyl groups on the adsorbent surface as indicated by Prauchner and Rodriguez-Reinoso (2012). The narrow, light peak at 1643.41cm^{-1} indicates carbon-carbon double bonds suggesting the presence of alkenes and amides, quinones or conjugated ketones i.e the characteristics of cellulose and hemi-celluloses as indicated by Sun and Webley (2010). The broad, light peak at 613.38 cm^{-1} indicates the presence of alkyne C-H bends and also suggests the presence of aliphatic bromo-compounds. A shallow peak at 2935.76 cm^{-1} indicates asymmetric/ symmetric stretches of methyl C-H groups. A 1247.99 cm^{-1} shallow peak indicates skeletal vibrations of C-C stretch while 1402.3 cm^{-1} indicates the presence of phenols or tertiary alcohols or carboxylate salts. The narrow, short peak at 1506.46 cm^{-1} indicates the presence of secondary amine bends (N-H).

3). Brunuaer, Emett and Teller (BET) Analysis

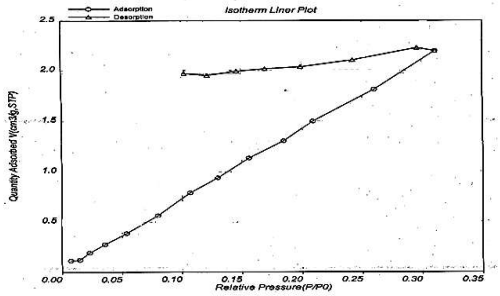

Fig.3. BET Micrograph for doum palm kernel

Analysis of the BET graph shows that the adsorption followed a linearized Type I Langmuir adsorption plot consistent with the prevailing isotherm model with a regression coefficient R^2 of 0.956457. The surface area of doum palm kernel powder by BET and Langmuir methods were found to be 13.464 and 31.246 m^2/g respectively with a pore volume of 0.309 cm^3. Analysis of the BET figures show that the quantity of nitrogen adsorbed (cm^3/g) increased with increase in the relative pressure (P/Po). However, the graph showed a desorption at a point as the pores became gradually filled up. The graphs corroborate the Langmuir formula which asserts a finite number of sites and greater monolayer adsorption of copper, iron and zinc ions than desorption. The graphs also indicate a hysteresis loop indicating capillary condensation occurring in mesoporous solids with a limit to uptake at high relative pressures. The shape of the hysteresis is related to the texture of the pore system as reported by Lowell *et al.* (2004). Analysis of the graph showed that the Barrett-Joyner-Halenda (BJH) average pore size for adsorption was 2.6 nm thus putting doum palm kernel in the class of mesoporous solids.

B. Pre-tannery wastewater characterization

Analysis of the pre-tannery wastewater showed initial concentrations of copper, iron and zinc ions at 1.5mg/L, 3.1mg/L and 0.81mg/L which were above the Nigerian Industrial Standard (NIS 2007). The effect of biosorbent dosage, contact time, agitation speed and temperature on removal or sorption of copper, iron and zinc ions from the pre-tannery wastewater were analyzed and optimum conditions deduced.

1). Effect of Biosorbent dosage

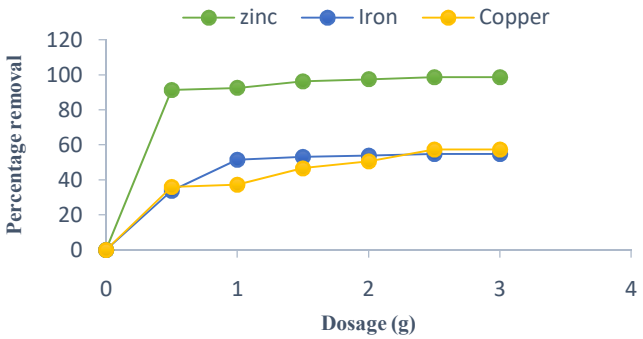

Fig. 4: Effect of biosorbent dosage on Cu^{2+}, Fe^{2+} and Zn^{2+} removal by Doum Palm (*HyphaeneThebaica)* kernel powder from Gombe pre-tannery wastewater at 100 rpm and 30 min.

From the Figure above, it can be observed that there was a steady increase in uptake of Copper, Iron and Zinc ions until the percentage uptake became constant at 57.33%, 54.84% and 98.76% of copper, iron and zinc ions respectively. The increase in metal uptake with increasing amounts of biosorbent is explained by the fact that at a fixed initial concentration of sorbate, the increase in the adsorbent amount provides a larger surface area or adsorptive sites (Vieira *et al.,* 2010). The constancy of the adsorbed amount per unit mass of adsorbent is attributed to the fact that a large adsorbent amount effectively reduces the unsaturation of the adsorption sites. Hence 2.5 g was taken as the optimum dosage.

2). Effect of Contact time

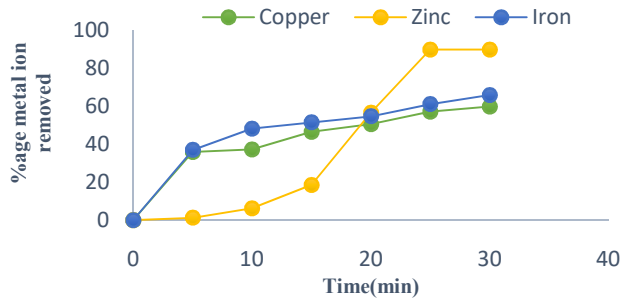

Fig.5: Effect of contact time (min) on percentage removal of Cu^{2+}, Fe^{2+} and $Zn^{2+}$from Gombe pre-tannery wastewater using Doum palm kernel powder:2.5 g dosage and 100 rpm.

Contact time plays an important role in the efficient removal of heavy metal ions using Doum palm kernel (*Hyphaenethebaica*). Analysis of Figure 5 showed that maximum adsorption was attained at 30mins contact time for the biosorbent at an optimum dosage of 2.5 g and 100 rpm mixing speed for the three metal ions under consideration hitting 56% for copper, 66% for iron and 90.12% for zinc ions respectively. The figure also showed that removal efficiency increased as the contact time increased from 0 to 30 min for the three metal ions thereby making 30 min the optimum contact time. For iron and copper ions the steep increase was a result of a larger adsorbent surface area which gradually reduced in size as most of the active sites got occupied thus leading to a nearly linear curve (Mohammed *et al.,* 2014). Adsorption is higher in the beginning as a result of the availability of a large number of active sites and adsorbent. As these sites get exhausted, the uptake rate is controlled by the rate at which the adsorbate is transported from the exterior to the interior sites of the adsorbent particles as indicated in Addagalla*et al.,* 2009.

3). Effect of Mixing speed

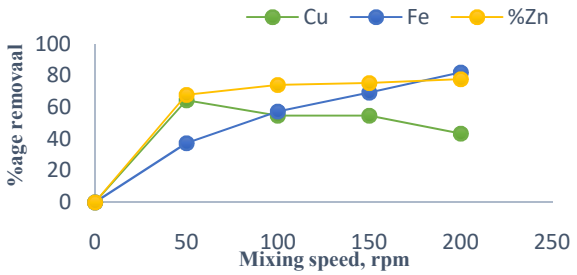

Fig. 6.Effect of mixing speed (rpm) on percentage removal of Cu^{2+}, Fe^{2+} and Zn^{2+}ions from Gombe pre-tannery wastewater using *H. Thebaica* (doum palm) kernel :2.5 g and 30 min.

Analysis of Figure 6 indicates that there was a steep increase in percentage uptake as the mixing speed increased from 0-50rpm for the three metal ions. These results can be associated with the fact that increase in agitation speed improves the diffusion of metal ions towards the surface of the adsorbent. It can also be observed that the removal efficiency for zinc and iron ions increased with increasing speed. However, for copper ion, there was a decrease in the percentage uptake. The removal efficiency was optimum at 50 rpm and began to decrease to roughly constant values at 100-150 rpm and began to decline at 200 rpm. This is due to the saturation of active sites with the adsorbate as mixing progressed.

4). Effect of temperature

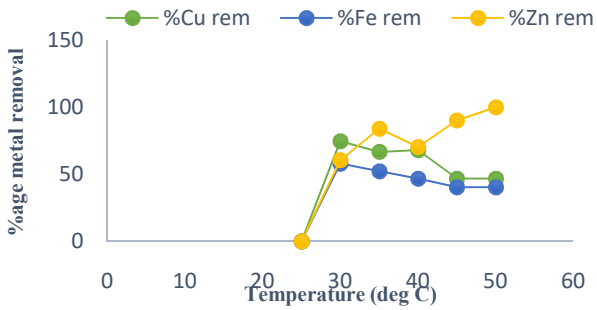

Figure 5: Effect of Temperature on Cu^{2+}, Fe^{2+} and Zn^{2+} removal from Gombe Pre-tannery wastewater by doum palm (*H. Thebaica*) kernel at 2.5 g dosage, 150 rpm, 30 min

It can be observed that there was a sharp rise in removal efficiency for the three metals from 0 to 60% for both iron and zinc and 75% for copper as the temperature increased from 25 ^{0}C to 30 ^{0}C suggesting that the adsorption was endothermic. It can also be attributed to an increase in the number of active sites available for biosorption on the biosorbent as well as a decrease in the viscosity of the liquid and the thickness of the boundary layer surrounding the biosorbent with increase in temperature accompanied by its positive effect on the mass transfer resistance of copper, iron and zinc ions. The same scenario was observed by Ogwuche *et al.,* (2015). Further observation of the figure above showed a decrease in the removal efficiency for Copper and iron as the temperature increased above 30 ^{0}C. This is due to deactivation or destruction of some of the active sites on the biosorbent surface. However, the efficiency of zinc removal increased to 100% at a higher temperature of 50 ^{0}C which could be due to the creation of new adsorption sites for the adsorption of zinc ions as well as affinity between the boundary layer and zinc ions in the remaining sites.

C. Thermodynamic Analysis of the biosorbent

Below are the relationships for copper, iron and zinc respectively

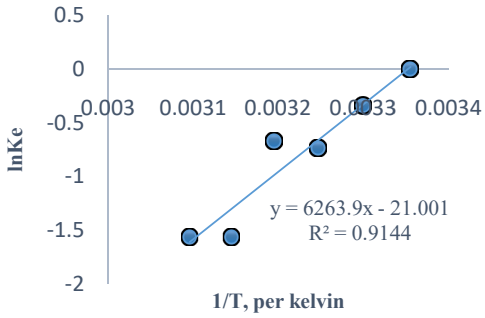

Fig.6. Thermodynamic relationship for the biosorption of Copper from Gombe Pre-tannery wastewaterby doum palm kernel.

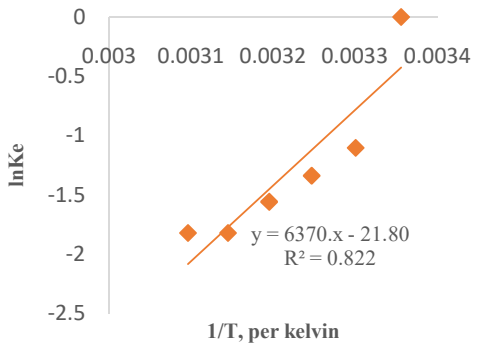

Fig.7. Thermodynamic relationship for the biosorption of iron from Gombe Pre-tannery wastewater by doum palm kernel.

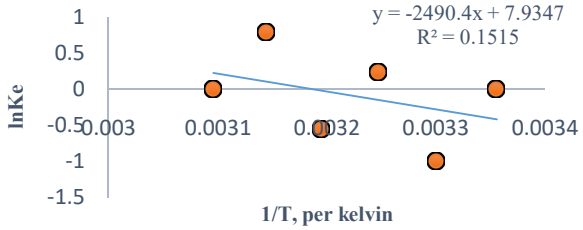

Fig. 8: Thermodynamic relationship for the sorption of zinc from Gombe pre-tannery wastewaterby doum palm kernel.

From Figure 6, the enthalpy of adsorption ΔH was calculated to be -52 kJ/mol showing that the biosorption of copper ions was exothermic implying that sorption of copper by doum palm kernel will be faster at lower temperatures. It also showed a very strong interaction between the doum palm kernel and the wastewater sample. Similarly, the entropy ΔS was found to be -0.174 kJmol^{-1}K^{-1}. The negative value of the entropy showed that heat was lost to the surrounding and the system was getting more stable. It was also observed that Gibb's free energy ΔG was positive showing non-spontaneity of the reaction which increased with increasing temperature. From Figure 7, the value of ΔH was deduced using the linearized equation to be -52.9 kJ/mol. The negative value of ΔH shows exothermic biosorption of iron by doum palm kernel. Entropy ΔS was calculated to be -0.181 kJmol^{-1}K^{-1}. The negative value of ΔS shows increasing stability of the system as temperature increased due to decreasing randomness of the sorbate-solution system as temperature increased. It also shows that the adsorption is chemical in nature with a weak forces of attraction and a decrease in randomness at doum palm/iron interface during the adsorption process (Atar*et al.,* 2012). There was an observed increase in the positive value ΔG with increasing temperature indicating that the system became less spontaneous as temperature increased. The exothermic nature of the system showed that biosorption of iron would be more efficient at much lower temperatures thus implying that lower temperatures would make the reaction more spontaneous. From the linearized equation in Figure 8, the enthalpy change ΔH was calculated to be 20.71 kJ/mol. The positive value of ΔH showed that sorption of zinc ions by doum palm kernel was endothermic. The low value of ΔH showed that it was a physical sorption (Vijayakumar *et al.,* 2012). The entropy change ΔS was also deduced to be 0.065 kJ/mol K. The positive value of ΔS showed increasing randomness of the solute-sorbate interaction as temperature increased. The value of ΔG was found to decrease and eventually became negative as the temperature increased from 25 ^{0}C to 50 ^{0}C as suggested by Malakootian *et al.*, 2008. This shows the thermodynamic favorability/feasibility and spontaneity of the sorption of zinc by doum palm kernel powder which increased with increasing temperature. From Figure 8, it can be deduced that

biosorption efficiency of zinc by doum palm would increase at higher temperatures. This is in agreement with Gaya *et al.,* 2015, Vijayakumar*et al.,* 2012 and Liu *et al.,* 2012 who worked on doum palm shell activated carbon, perlite and sesame leaf biosorbents respectively. The positive value of ΔS showed affinity of the doum palm kernel for zinc.

D. *Adsorption Isotherms*

From Table 1 below, the Langmuir sorption isotherm fit the experimental data for copper and zinc thus showing monolayer adsorption with a finite number of sites. Sorption of iron however followed Temkin isotherm which showed a linearly exponential distribution of energy of adsorption.

TABLE 1
EVALUATED THERMODYNAMIC DATA FOR SORPTION OF COPPER, IRON AND ZINC IONS BY DOUM PALM KERNEL

Metal ion	ΔH kJ/mol	ΔS kJ/mol	ΔG (kJ/mol)					
			298K	303K	308K	313K	318K	323K
Copper	-52.1	-0.174	46.6	-826.44	-1699.45	-2572.46	-3445.47	-4318.48
Iron	-52.9	-0.181	1058.3	-1964.70	-2871.09	-3777.48	-4683.87	-5590.27
Zinc	+20.7	+0.066	-1046.4	-716.55	-386.70	-56.86	+272.99	+602.83

D. Adsorption Isotherms

TABLE 2
EVALUATED CONSTANTS FOR LANGMUIR, FREUNDLICH AND TEMKIN ISOTHERMS

Parameter	Isotherm	K_L (l/mg)	K_F (l/g)	Q_m (mg/g)	n_F	B_T (J/mol)	A_T (l/g)	b_T	R^2
Copper	Langmuir	-0.669	-	0.25	-	-	-	-	0.9417
	Freundlich	-	2.120	-	*0.5106*	-	-	-	0.9025
	Temkin	-	-	-	-	0.0807	0.0426	*30701*	0.0159
Iron	Langmuir	0.0726	-	4.38	-	-	-	-	0.6451
	Freundlich	-	0.373	-	*0.9124*	-	-	-	0.4402
	Temkin	-	-	-	-	1.84	0.9606	*1347*	0.8476
Zinc	Langmuir	16.23	-	1.19	-	-	-	-	0.9022
	Freundlich	-	1.649	-	*6.4641*	-	-	-	0.1035
	Temkin	-	-	-	-	0.0675	0.1943	*36705*	0.1656

1) Adsorption Kinetics

TABLE 3
EVALUATED CONSTANTS FOR ADSORPTION KINETICS FOR SORPTION

Parameter	Kinetic Model	R^2	Intercept	Slope	Rate constant K	Diffusion Constant mg/g min	qe (mg/g)
Copper	Pseudo first order	0.5331	0.1327	-0.0595	0.1370 (min^{-1})	-	1.357
	Pseudo second order	0.9830	-12.488	6.6882	3.582 (g/mg min)	-	0.149
Iron	Pseudo first order	0.1184	-1.0481	-0.0225	0.0518 (min^{-1})	-	0.0895
	Pseudo second order	0.9909	3.283	2.338	1.665 (g/mg min)		0.4277
	Intra-particle Diffusion model	0.8670	0.0604	0.0754	-	0.0754	-
Zinc	Pseudo first order	0.897	0.1767	-0.0549	0.126 (min^{-1})	-	0.6657
	Pseudo second order	0.1805	977.61	-28.713	0.843 (g/mg min)		0.0348
	Intra-particle Diffusion model	0.6916	-0.0483	0.0351	-	0.0351	-

Analysis of Table 6above shows that the sorption of copper and zinc ions followed pseudo-second order kinetics with chemisorption being the rate limiting step while that of iron followed pseudo-first order.

2) *Error Functions for Isotherms*

TABLE 4
ERROR FUNCTIONS FOR ISOTHERMS

Isotherm model	R^2	APE%	X^2	MPSD	RMS	RMSD
Copper						
Langmuir	0.9417	91.074	-585.979	2447.131	91.167	226.793
Freundlich	0.9025	13.686	1.183	108.784	43.348	0.408
Temkin	0.0159	0.736	0.916	95.711	72.246	0.182
Iron						
Langmuir	0.6451	89.688	38.168	617.802	89.867	6.599
Freundlich	0.4402	4.911	1.899	137.837	52.732	0.544
Temkin	0.8476	17.836	2.259	150.298	44.969	0.773
Zinc						
Langmuir	0.9022	15.357	1.268	112.583	43.409	0.432
Freundlich	0.1035	91.729	23.435	484.102	84.736	3.713
Temkin	0.1656	1.076	1.773	133.145	95.033	0.277

Analysis of the table above showed that sorption followed Langmuir isotherm for copper, Freundlich for iron and Temkin for zinc.

IV. CONCLUSION

Doum palm kernel was prepared with moisture and oil removed to ensure proper characterization. Wastewater from Gombe pre-tannery was characterized for the presence of copper, iron and zinc ions. Jar tests conducted indicated an optimum dosage of 2.5 g, optimum mixing time of 30 min, mixing speed at 150 rpm and optimum temperature 50 ^{0}C. XRF analysis of Doum palm indicated a high concentration of pottasium known for its reactivity. SEM analysis revealed a rough, non-homogenous surface with voids, crevices which indicate the surface of Doum palm fits that of a good biosorbent and will facililtate easy sorption and diffusion. With a BET area of 13.46 m^2/g and Langmuir surface of 31.46 m^2/g and pore width of 2.6 nm thereby putting doum palm kernel in the class of mesoporous solids coupled with an appreciable reduction of copper, iron and zinc ions from Gombe pre-tannery wastewater, it can be concluded that doum palm kernel is a good biosorbent which can be used as a viable and less costly alternative in the reduction of heavy metal ions from wastewater before disposal.

ACKNOWLEDGEMENT

The authors acknowledge the support of Tertiary Education Trust Fund (TETFUND) in carrying out this research work.

REFERENCES

[1]. Addagalla V. A, Naif, A. D and Nidal, H. (2009); Study of Various Parameters in the Biosorption of Heavy Metalson Activated Sludge. World Applied Science Journal, *5.* 32-40.

[2]. Adekola F. A., Hodonou D. S. S and Adegoke H. I. (2016); Thermodynamic and Kinetic Studies of Biosorption of Iron and Manganese from Aqueous Medium using Rice Husk Ash, Applied Water Science 6: 319-330.

[3]. Ahalya N., Kanamadi R. D. and Ramachandra T. V. (2003); Biosorption of Heavy Metals, Research Journal of Chemistry and the Environment 7, 71-78.

[4]. Aharoni. C. and Ungarish. M (1977); Kinetics of Activated Chemisorptions. Part 2. Theoretical models.Journal of Chemical Society Faraday Trans. 73. 456–464.

[5]. Atar, N., Olgun, A. and Wangb, S. (2012); Adsorption of Cadmium (II) and Zinc (II) on Boron Enrichment Process Waste in Aqueous Solutions: Batch and Fixed-Bed System Studies, Chemical Engineering Journal,192, 1- 7, http://dx.doi.org/10.1016/j.cej.2012.03.067

[6]. Awwad A. and Salem N. (2011); Kinetics and Thermodynamics of Cd (II) Biosorption onto Loquat (*Eriobotrya Japonica*) leaves, Journal of Saudi Chemical Society,

[7]. Babák L., Šupinová P., Zichová M., Burdychová R. and Vítová E. (2012); Biosorption of Cu, Zn and Pb by Thermophilic Bacteria – Effect of Biomass Concentration on Biosorption Capacity, ActaUniversitatisAgriculturae Et SilviculturaeMendelianaeBrunensis LX 1 (5),2-6.

[8]. Basha S, Murthy Z. V. P. and Jha B. (2009); Sorption of Hg(II) onto *Carica papaya*: Experimental Studies and Design of Batch Sorber. Chemical Engineering Journal, 147:226–234.

[9]. Bhattacharya A. K, Mandal S. K. and Das S. K (2006); Adsorption of Zn (II) from Aqueous Solutions by Using Different Adsorbents, Chemical Engineering Journal, 123:43–51.

[10]. Butterworth R.F (2010); Metal Toxicity, Liver disease and Neurodegeneration, Neurotoxic Research 18:100-105.

[11]. Chakraborty, S. De, S., Das Gupta, S. and Basu, J.K. (2005); Adsorption Study for the Removal of a Basic Dye: Experimental and Modeling. Chemosphere, 58(8), 1079-1086.

[12]. Chan L.S, Cheung W. H, Allen S. J and McKay G. (2012); Error Analysis of Adsorption Models for Acid Dyes onto Bamboo

Derived Activated Carbon, China Journal of Chemical Engineering. 20(3), 535-542

[13]. El-Nafaty U. A, Muhammad I. M and Abdulsalam S. (2013); Biosorption and Kinetic studies on Oil Removal from Produced Water using Banana Peel. Civil and Environmental Research, 3(7), 4-7.

[14]. El-Sadaawy M., Abdelwahab O. (2014); Adsorptive removal of Nickel from Aqueous Solutions by Activated Carbons from Doum Palm Seed Coat. Alexandria Engineering Journal, 53, 399-408.

[15]. Faller P. (2009); Copper and Zinc Binding to Amyloid-beta: Coordination, Dynamics, Aggregation, Reactivity and Metal-ion Transfer, Chemical Biochemistry, 10 (18):2837-45.

[16]. Freundlich H. M. (1906); Over the adsorption in solution. Z. Phys. Chem. 57, 385–470.

[17]. Gaya. U.I, Emmanuel O. and Abdul Halim A. (2015); Adsorption of Aqueous Cd (II) and Pb (II) on Activated Carbon Nanopores prepared by Chemical Activation of Doum Palm Shell. SpringerPlus vol. 4, 3-5.

[18]. Hall K. R., Eagleton L. C., AcrivosA.Vermeulen T. (1966); Pore- and Solid-Diffusion Kinetics in Fixed-Bed Adsorptionunder Constant-Pattern Conditions, I&EC Fundam. V, 212–223.

[19]. Hameed B. H, Krishni R. R and Sata S. A (2009); A Novel Agricultural Waste Adsorbent for the Removal of Cationic Dye from Aqueous Solutions, Journal of Hazardous materials, 162(1),305-311.

[20]. Ho, Y.S. (2006a); Review of Second-Order Models for Adsorption Systems, Journal of Hazardous Materials, *136(3)*, 681–689.

[21]. Ho Y.S. and McKay G. (1999); Pseudo-second order model for sorption processes, Process Biochemistry,34(5), 451–465.

[22]. Hureau C., Faller P. (2009); A Beta-mediated ROS Production by Cu ions: Structural Insights, Mechanisms and Relevance to Alzheimer's disease, Biochimie. 91 (10):1212-1213.

[23]. Kalavathy M. H., Karthikeyan T., Rajgopal S., Miranda L. R. (2005); Kinetic and Isotherm Studies of Cu(II) Adsorption onto H_3PO_4– Activated Rubber Wood Sawdust, Journal of Colloid Interfibrillary Science, 292, 354–362.

[24]. Langmuir I. (1918); The Adsorption of Gases on Plane Surfaces of Glass, Mica and Platinum, Journal of American Chemical Society 40, 61–1403.

[25]. Lesmana S.O., Febriana N., Setaredjo N., Sunarso J., Ismadji S (2009); Studies on Potential Applications of Biomass for the Separation of Heavy Metals from Water and Wastewater, Biochemical Engineering Journal 44:19–41.

[26]. Li-e Liu, Jindun L., Hongping Li, Haoqin Z., Jie L and Hongquan Z. (2012); Equilibrium, Kinetic and Thermodynamic Studies of Lead (II) Biosorption on Sesame Leaf, BioResources 7(3),3555-3572.

[27]. Lowell, S., Shields, J.E., Thomas, M.A. and Thommes, M (2004); Characterization of PorousSolidsand Powders:Surface Area, Pore Size and Density, Kluwer Academic Publishers, The Netherlands, pp 11-20.

[28]. Malakootian M., Almasi A., Hanoi H. (2008); Lead (Pb) and Cobalt Removal from Paint Industries Effluent Using Wood Ash, International Journal of Environmental Science and Technology 5(2):217–222.

[29]. Mercer J. F.B. (2001); The Molecular Basis of Copper-transport Diseases, Trends in Molecular Medicine 7:64-69.

[30]. Mishra V. (2014); Biosorption of Zinc ion: A Deep Comprehension, Applied Water Science 4:311-332.

[31]. Mohammed, J., Nasri, N.S., Zaini, A.A.M., Hamza, U.D., Ahmed, M.M. (2014); Optimization and Preparation of Microwave Irradiated Bio-based Materials as Porous Carbons for VOCs Removal using Response Surface Methodology, Applied Mechanics of Materials 5(54), 175-179.

[32]. Monisha J., Tenzin T., Naresh A., Blessy B. and Krishnamurthy N. B. (2014); Toxicity, Mechanism and Health Effects of some Heavy metals, Journal of Interdisciplinary Toxicology 7(2): 60-72.

[33]. Muhammad I. M, El-Nafaty U. A, Abdulsalam S and Makarfi Y. I. (2012); Removal of Oil from Oil producedwaterusing Eggshell, Civil and Environmental Research, Journal of International Institute for Science, Technology and Education, 2 (8) 52-61.

[34]. Norton L., Baskaran K. and McKenzie S T. (2004); Biosorption of Zinc from Aqueous Solutions using Bio-solids, Advanced Environmental Research 8: 629-635.

[35]. Ogwuche E. O, Gimba C. E and Abechi, E. S (2015); An Evaluation of the Adsorptive Behaviour of Activated Carbon Derived from *Hyphaenethebaica* Nut shells for the Removal of Dichlorvos from Wastewater. The International Journal of Science and Technology ISSN 2321-919X., 3(4): 2-7.

[36]. Plazinski W., Rudzinski W., Plazinska A. (2009); Theoretical Models of Sorption Kinetics Including a Surface Reaction Mechanism: A Review, Advanced Colloid Interface Science, 152(1–2), 2–13.

[37]. Reddy D.H.K, Seshaiah K, Reyddy A.V.R, Rao M.M & Wang M. C. (2010). Biosorption of Pb^{2+} from Aqueous Solutions by *Moringaoleifera* bark: Equilibrium and Kinetic Studies, Journal of Hazard Materials 174, 831–838.

[38]. Struzynska L. (2009). A Glutamatergic Component of Lead Toxicity in Adult Brain: The Role of Astrocytic Glutamate Transporters, Neurochemistry International, 55:151-156.

[39]. Sun, Y. and Webley, P.A. (2010; Preparation of Activated Carbons from Corncob with Large Specific Surface Area by a Variety of Chemical Activators and their Application in Gas Storage, Chemical Engineering Journal, 162, 883-892.

[40]. Tan J., Xiaoyu Z., Xinhao W. and Lijuan W. (2012); Removal of Malachite Green from Aqueous Solutions using Waste Newspaper Fibre, BioResources 7(3), 4307-4320.

[41]. Vieira M. G. A, Neto A. F. A, Gimenes M. L, and Da Silva M.G.C. (2010); Sorption Kinetics and Equilibrium for the Removal of Nickel Ions from Aqueous Phase On Calcined Bofe /Bentonite Clay. Journal of Hazardous Materials 177, 362–371.

[42]. Vijayakumar G., Tamilarasan R. and Dharmendirakumar M. (2012); Adsorption, Kinetic, Equilibrium and Thermodynamic Studies on the Removal of basic dye Rhodamine from Aqueous Solution by the Use of Natural Adsorbent Perlite, Journal of Material and Environmental sciences, 3(1), 157-170

[43]. Vilar V.J.P., Botelho C.M.S. and Boaventura R.A.R. (2007; Chromium and Zinc Uptake by Algae *Gelidium*and Agar Extraction Algal Waste: Kinetics and Equilibrium, Journal of Hazardous Materials, 149:643–649

[44]. Visnjic-Jeftic Z., Jaric I., Jovanovic L., Skoric S., Smederevac-Lalic M., Nikcevic M., Leonhard M. (2010); Heavy Metal and Trace Element Accumulation in Muscle, Liver and Gills of the Pontic Shad (*Alosa Immaculate Bennet 1835*) from the Danube River (Serbia), Microchemistry Journal, 95:341-344.

[45]. Weber W. J. and Morriss J. C. (1963); Kinetics of Adsorption on Carbon from Solution, Journal of Sanitary Engineering Division of the American Society of Civil Engineering, 89(1963) 31–60.